



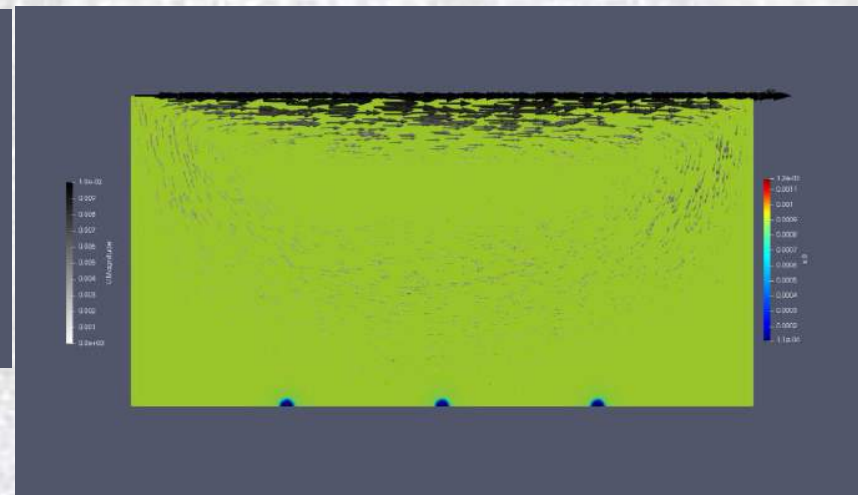
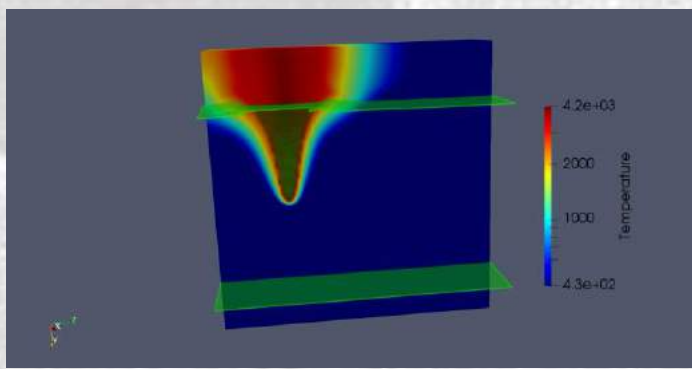
Recent Developments in Mathematical Modelling Frameworks for Computational Metallurgy

Computational Metallurgy in the Solid, Liquid, Vapour and Plasma States

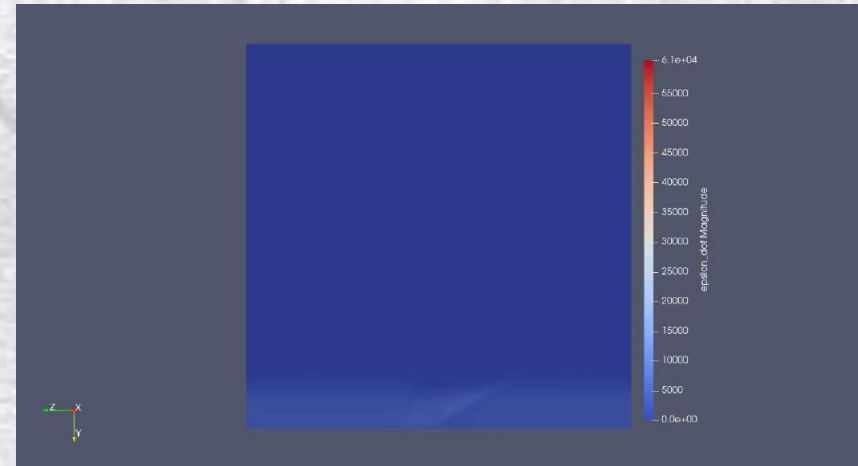
Dr Tom Flint

The University of Manchester

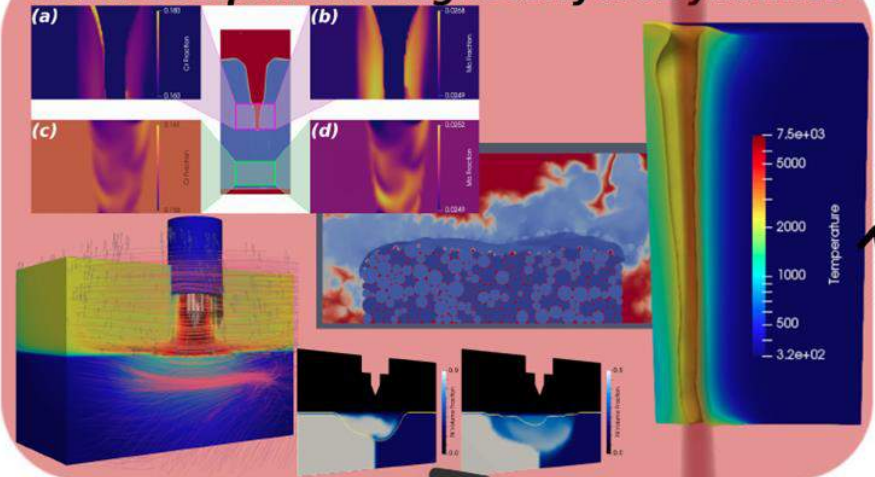
Contents



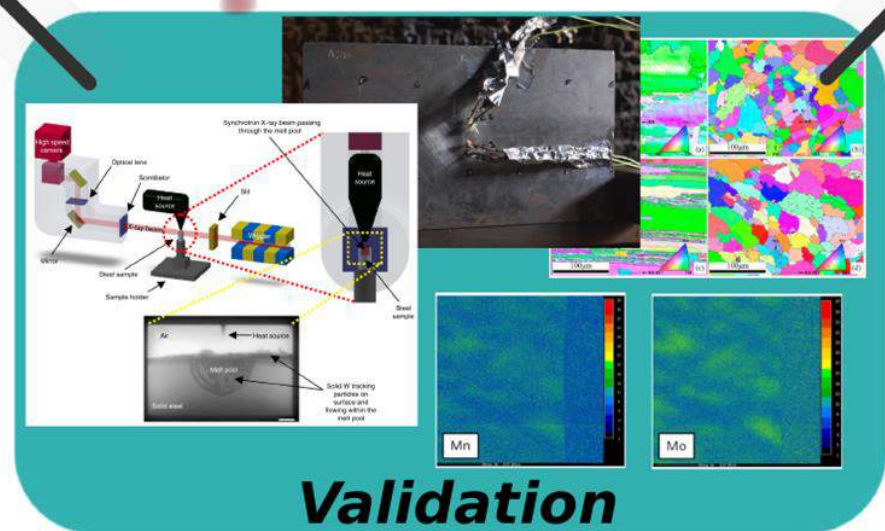
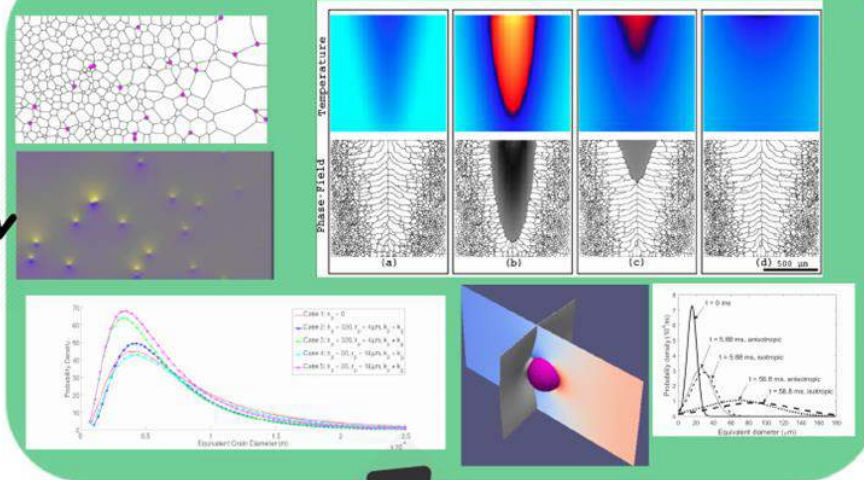
- **Thermal-Fluid Dynamics**
 - Multi-Component Thermal-Fluid-Dynamics with state transformations
 - Simplifications for computational tractability & Open-Source
 - beamweldFoam, laserbeamFoam, laserbeamFoam V2
 - Heterogeneous Magnetohydrodynamics
- **Microstructural Evolution**
 - Multi-Component Multi-Phase Field Formulations for microstructural evolution
 - Simplifications for computational tractability
 - Single component multiphase
- **Solid Dynamics**
 - Eulerian Crystal Plasticity for High Strain Rate and Coupled Microstructural Solid Mechanics Problems



Multi-Component MagnetoHydroDynamics



Microstructural Evolution Kinetics

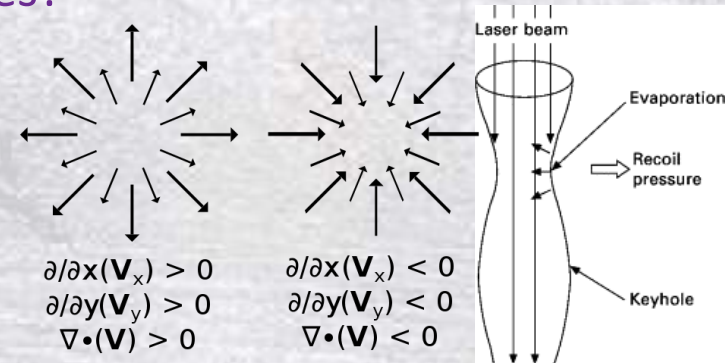
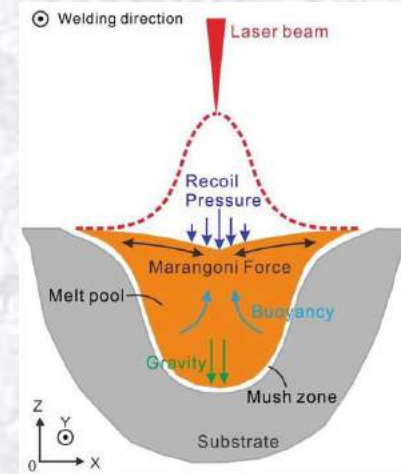


Validation

Research Background

It is Important to Understand the Flow Physics in Conjunction with the Solid-State Physics

- What happens when an alloy melts?
 - Surface Tension
 - Temperature Dependence of Surface Tension
 - Buoyancy
 - Lorentz Force in case of Electromagnetically (Arc) driven processes
 - Laser-Substrate Interactions
 - $\nabla \cdot \mathbf{U} = 0$
- Additionally, what happens when an alloy vaporises?
 - Vaporisation of substrate causes ~3 order of magnitudes change in density
 - Massive volumetric expansion
 - $\nabla \cdot \mathbf{U} \neq 0$
 - Certain alloying elements vapourise more easily and the substrate experiences preferential evaporation



$$\begin{aligned} \frac{\partial}{\partial x}(\mathbf{V}_x) &> 0 \\ \frac{\partial}{\partial y}(\mathbf{V}_y) &> 0 \\ \nabla \cdot (\mathbf{V}) &> 0 \end{aligned}$$

$$\begin{aligned} \frac{\partial}{\partial x}(\mathbf{V}_x) &< 0 \\ \frac{\partial}{\partial y}(\mathbf{V}_y) &< 0 \\ \nabla \cdot (\mathbf{V}) &< 0 \end{aligned}$$

Multi-Component Thermal Fluid Dynamics

Highlights

$$\frac{\partial(\rho \mathbf{U})}{\partial t} + \nabla \cdot (\rho \mathbf{U} \otimes \mathbf{U}) = -\nabla P + \nabla \cdot \boldsymbol{\tau} + \mathbf{F}_s + \mathbf{F}_g + \mathbf{S}_m$$

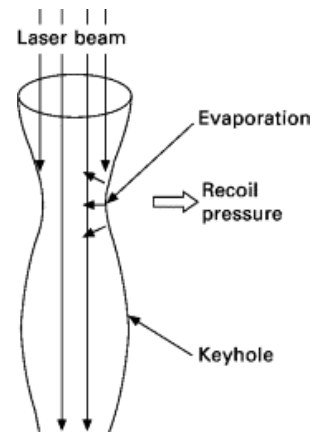
$$\frac{\partial(\rho c_p T)}{\partial t} + \nabla \cdot (\mathbf{U} c_p \rho T) - \nabla \cdot (k \nabla T) = q + \boldsymbol{\tau} : \nabla \mathbf{U} - L_f \left[\frac{\partial(\rho \epsilon_1)}{\partial t} - \nabla \cdot (\mathbf{U} \epsilon_1 \rho) \right] - L_v \dot{m}_T$$

$$\frac{\partial(\rho_k \alpha_k)}{\partial t} + \nabla \cdot (\rho_k \mathbf{U} \alpha_k) = \nabla \cdot \left(\rho D_k \nabla \left(\frac{\rho_k \alpha_k}{\rho} \right) \right) + \dot{m}_k$$

$$\frac{\alpha_k}{\rho} \frac{D\rho}{Dt} = \alpha_k \nabla \cdot \mathbf{U}$$

$$\frac{D\rho}{Dt} = \frac{\partial\rho}{\partial t} + \mathbf{U} \cdot \nabla \rho$$

- Developed new descriptions of alloy substrates experiencing fusion and vapourisation state transitions.
- **Explicitly captures volumetric dilation due to density changes through vapourisation/condensation transition**
- My framework is multi-component – incorporates diffusive fluxes between components in the system
- **Only framework that fully describes alloy systems in the fluid states**
- Others use phenomenological models for recoil at vapourisation and are only single-component
- Other approaches assume divergence free velocity field – Incorrect for additive manufacturing & power beam scenarios
- **Evaporation of elements is fully described by my framework**
- Complete description of multi-component flow in high energy density processes – No magnetic fields in power beam processes



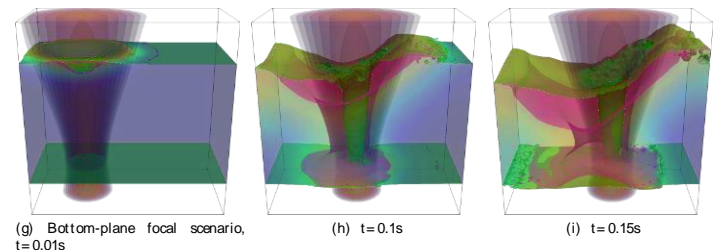
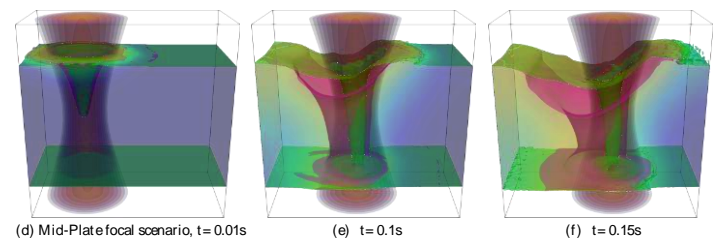
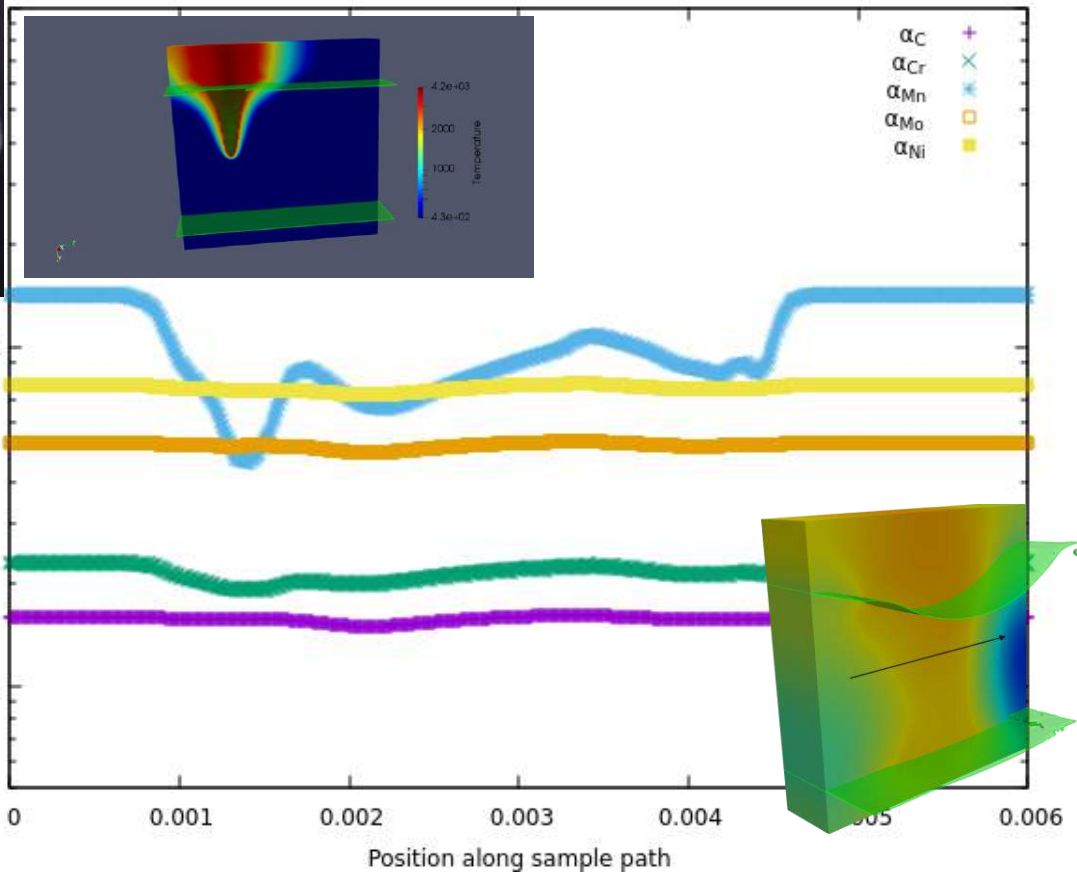
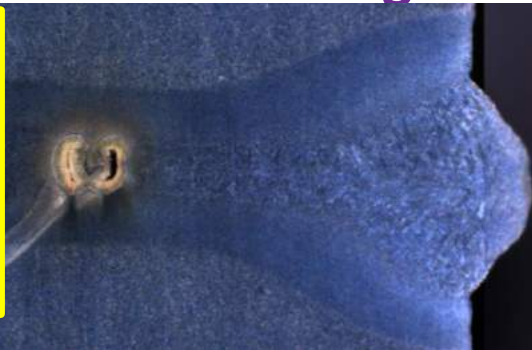
Keyhole Stability

Porosity Mitigation

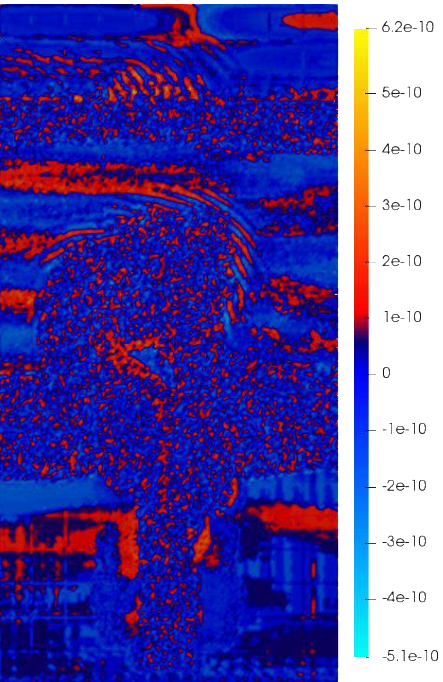
Flint, T.F., Scotti, L., Basoalto, H.C. et al. A thermal fluid dynamics framework applied to multi-component substrates experiencing fusion and vaporisation state transitions. *Commun Phys* 3, 196 (2020).

Applications – NAMRC: Numerical Tuning of Beam Processing Conditions to Minimize Porosity Formation

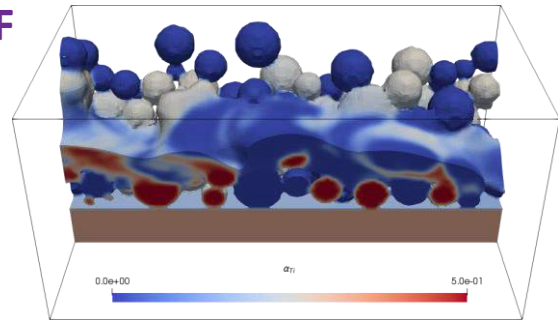
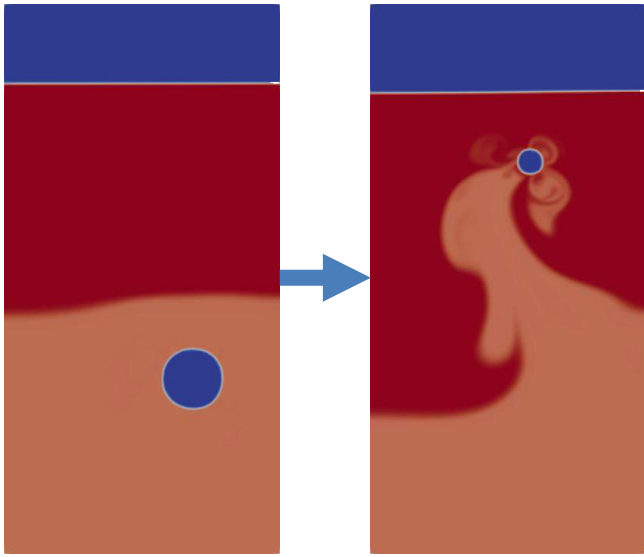
T.F. Flint, et al, A fundamental investigation into the role of beam focal point, and beam divergence, on thermo-capillary stability and evolution in electron beam welding applications, International Journal of Heat and Mass Transfer, 2023



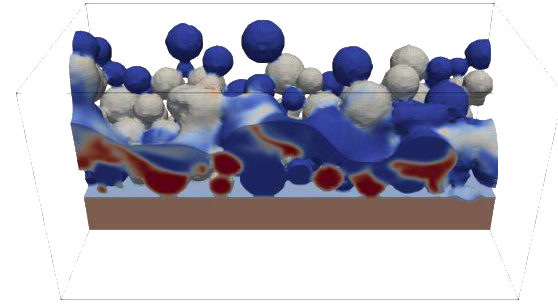
Applications – Effect of condensation in mixing during L-PBF



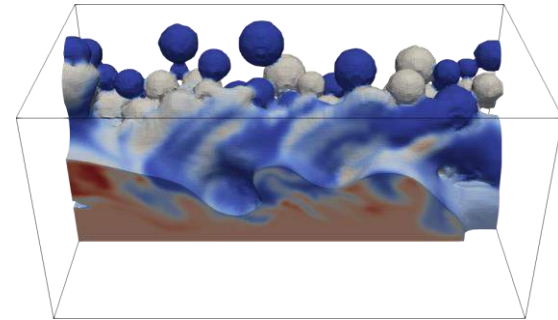
$$\frac{\partial \rho}{\partial t} + \nabla \cdot (\rho U)$$



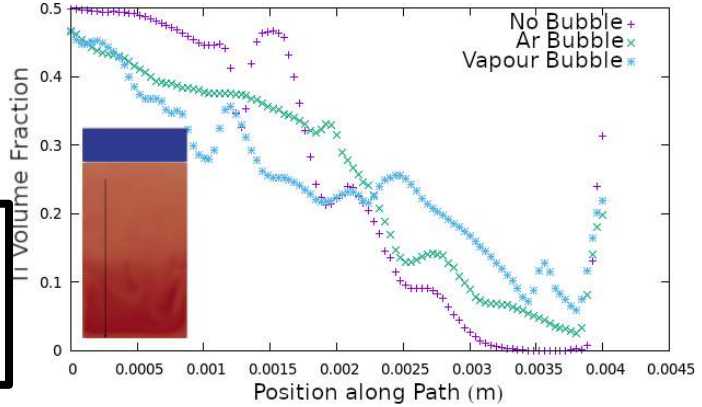
(a) Case 1



(b) Case 2



(c) Case 3



Increased Power Density

T.F. Flint, et al, **A fundamental analysis of factors affecting chemical homogeneity in the laser powder bed fusion process**, International Journal of Heat and Mass Transfer,

The Two Approaches used in the Presented Work

- Both approaches solve a momentum conservation and energy conservation equation
 - Accounting for buoyancy, solidification and surface tension effects in the momentum equation
 - Includes latent heats of vapourisation and fusion in energy equation
- Both approaches have been validated against Gallium Melting case and the Sen and Davies Marangoni flow case
- Flint et al vaporisation implementation validated against vapour bubble growth case
- Differences are
 - 1.) The treatment of the vaporisation state transition
 - 2.) MULES vs ISO-Advecting for interface

$$\frac{\partial(\rho\mathbf{U})}{\partial t} + \nabla \cdot (\rho\mathbf{U} \otimes \mathbf{U}) = -\nabla P + \nabla \cdot \boldsymbol{\tau} + \mathbf{F}_s + \mathbf{F}_g + \mathbf{S}_m$$

$$\frac{\partial \rho c_p T}{\partial t} + \nabla \cdot (\mathbf{U} c_p \rho T) - \nabla \cdot (k \nabla T) = q + S_h$$

Flint et al.

In the approach by Flint et al. the volumetric change going from a liquid metal to less dense vapour is explicitly captured and produces an extra term in the pressure equation associated with the material derivative of density – this approach by Flint et al. fully conserves mass and can be applied to N component mixtures experiencing fusion and vaporisation transitions.

$$\boldsymbol{\tau} = \mu \left[\nabla \mathbf{U} + (\nabla \mathbf{U})^T \right] - \frac{2}{3} \mu (\nabla \cdot \mathbf{U}) \mathbf{I}$$

$$\frac{\partial(\rho_k \alpha_k)}{\partial t} + \nabla \cdot (\rho_k \mathbf{U} \alpha_k) = \nabla \cdot \left(\rho D_k \nabla \left(\frac{\rho_k \alpha_k}{\rho} \right) \right) + \dot{m}_k$$

$$\nabla \cdot \left(\frac{1}{A_D} \nabla p \right) = \nabla \cdot \phi - \dot{v}$$

MULES

Parivendhan et al.

The vaporisation transition is modelled by neglecting the volumetric change induced going from liquid to metallic vapour – this allows the more convenient divergence free velocity field closure to be applied. However, a phenomenological recoil pressure term must then be added to account for the missing volumetric dilation information in the framework.

α_1 =metal phase, α_2 =Argon phase

$$\nabla \cdot \mathbf{U} = 0$$

$$\boldsymbol{\tau} = \mu \left[\nabla \mathbf{U} + (\nabla \mathbf{U})^T \right] \quad \frac{\partial \alpha}{\partial t} + \nabla \cdot (\alpha \mathbf{U}) = 0$$

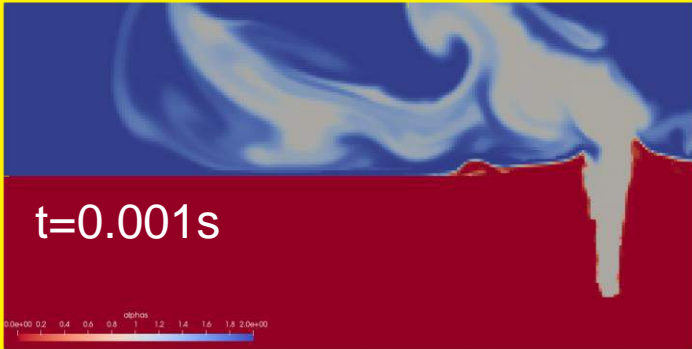
ISO-Advecting

$$p_v(T) = p_0 \exp \left\{ \frac{\Delta H_v}{R} \left(\frac{1}{T_v} - \frac{1}{T} \right) \right\}$$

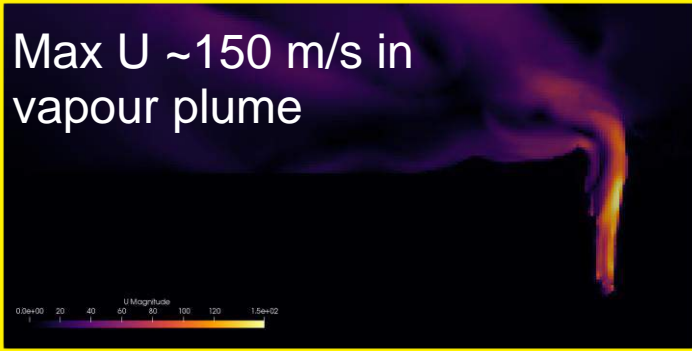
Multi-Component Thermal Fluid Dynamics

Differences between my framework and state of the art

Flint *et al.*



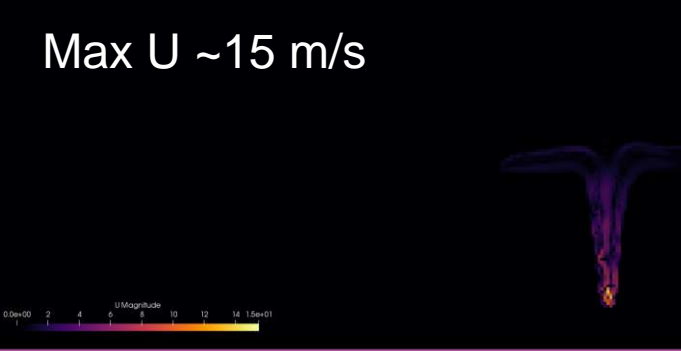
Max U ~150 m/s in
vapour plume



Previous state of the art



Max U ~15 m/s



Largest criticism of modelling of welding, additive manufacturing and other joining processes is that they do not predict the correct large magnitude velocity fields measured experimentally

This is due to the neglect in other approaches of the volume increase/decrease due to vapourisation/condensation respectively

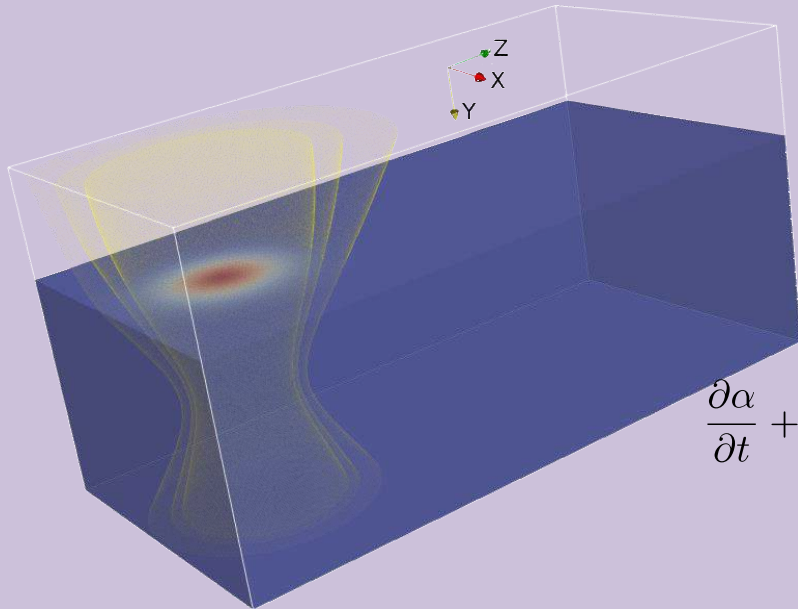
The change in density during vapourisation largely determines the flow dynamics in advanced manufacturing processes

Open-Source Thermal Fluid Dynamics Implementations

Electron-beam substrate interactions

<https://github.com/tomflint22/beamWeldFoam>

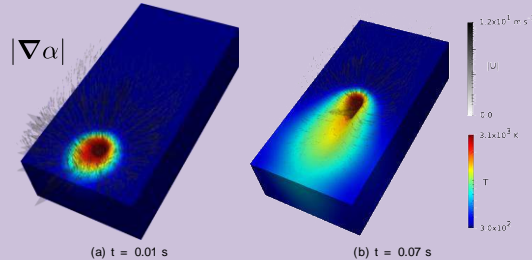
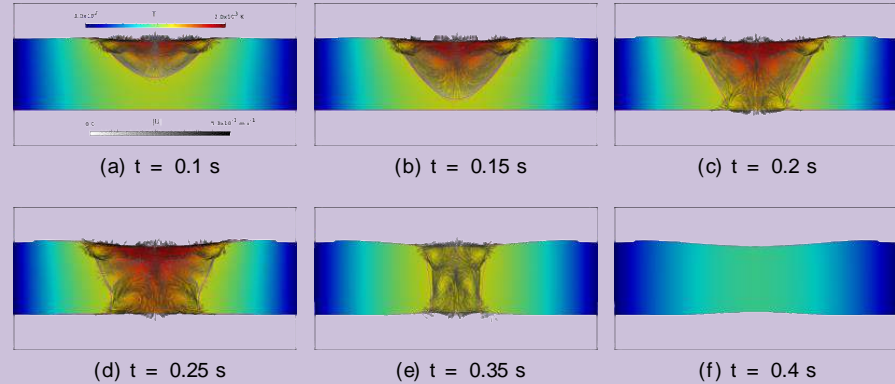
- Includes circular beam oscillation with translation



$$\mathbf{F}_s = \left[(\sigma\kappa + P_v)\hat{n} + \frac{d\sigma}{dT} (\nabla T - (\hat{n} \cdot \nabla T)\hat{n}) \right] |\nabla\alpha|$$

$$\frac{\partial\alpha}{\partial t} + \nabla \cdot (\alpha\mathbf{U}) = 0$$

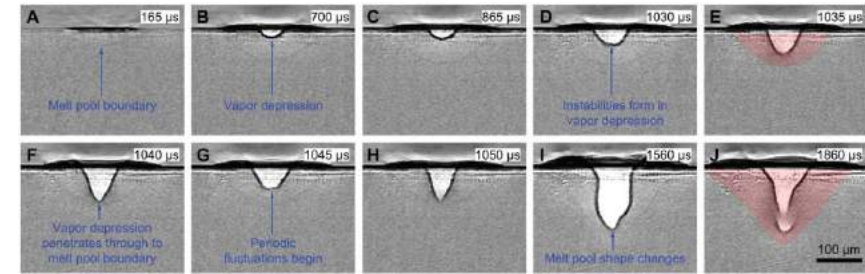
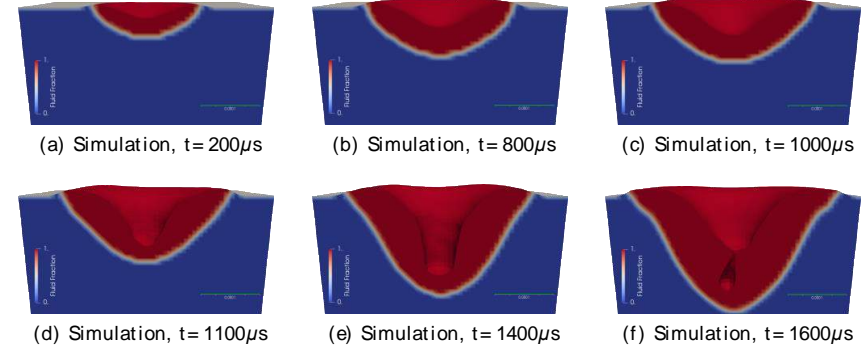
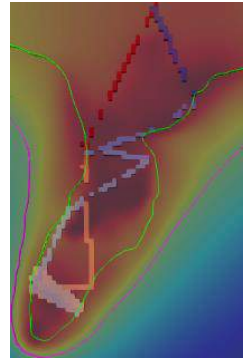
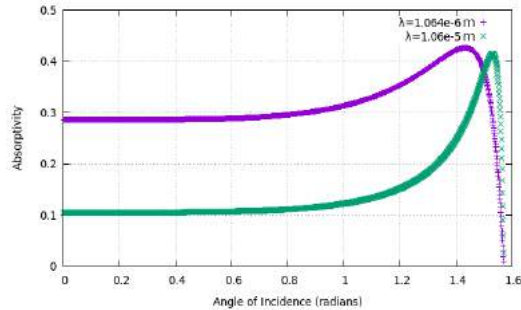
$$\nabla \cdot \mathbf{U} = 0$$



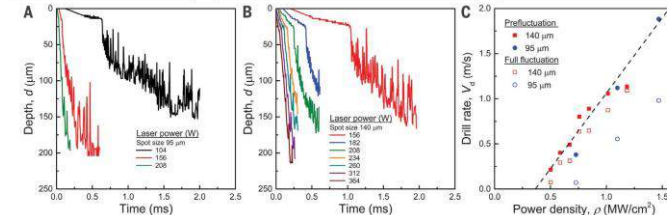
Thomas F. Flint, Gowthaman Parivendhan, Alojz Ivankovic, Michael C. Smith, Philip Cardiff, **beamWeldFoam**: Numerical simulation of high energy density fusion and vapourisation-inducing processes, SoftwareX, Volume 18,

<https://github.com/micmog/LaserbeamFoam>

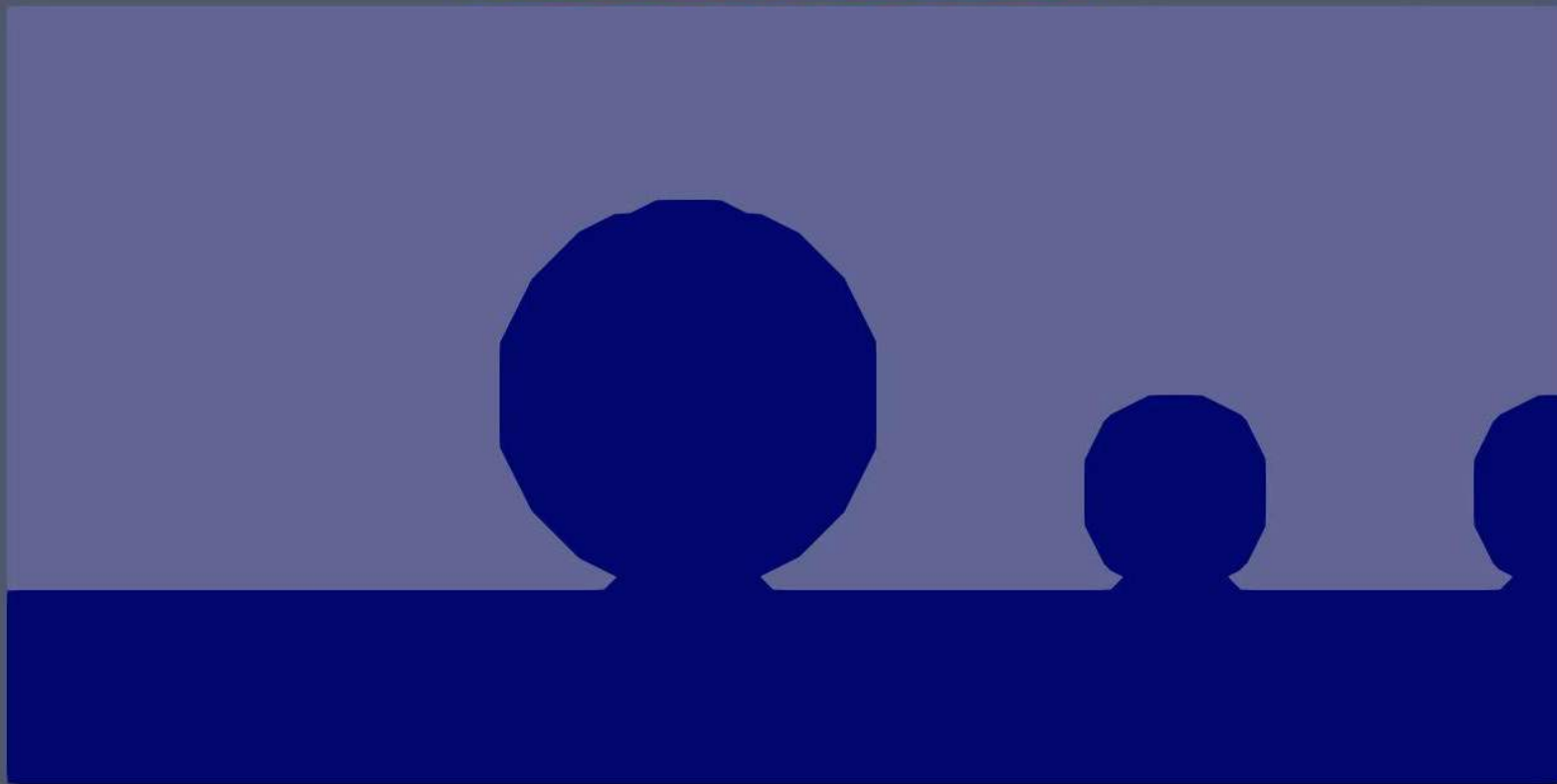
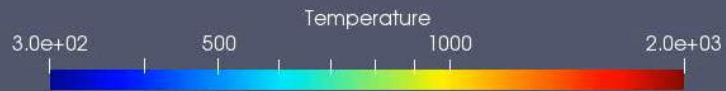
- The laser ray-tracing implementation works by discretising the laser beam into N individual 'Rays'
- These individual Rays are then tracked through the domain, until they meet the liquid/gas interface
- At this point, the absorptivity is calculated and the fraction of energy for the given Ray is deposited and the remainder is reflected

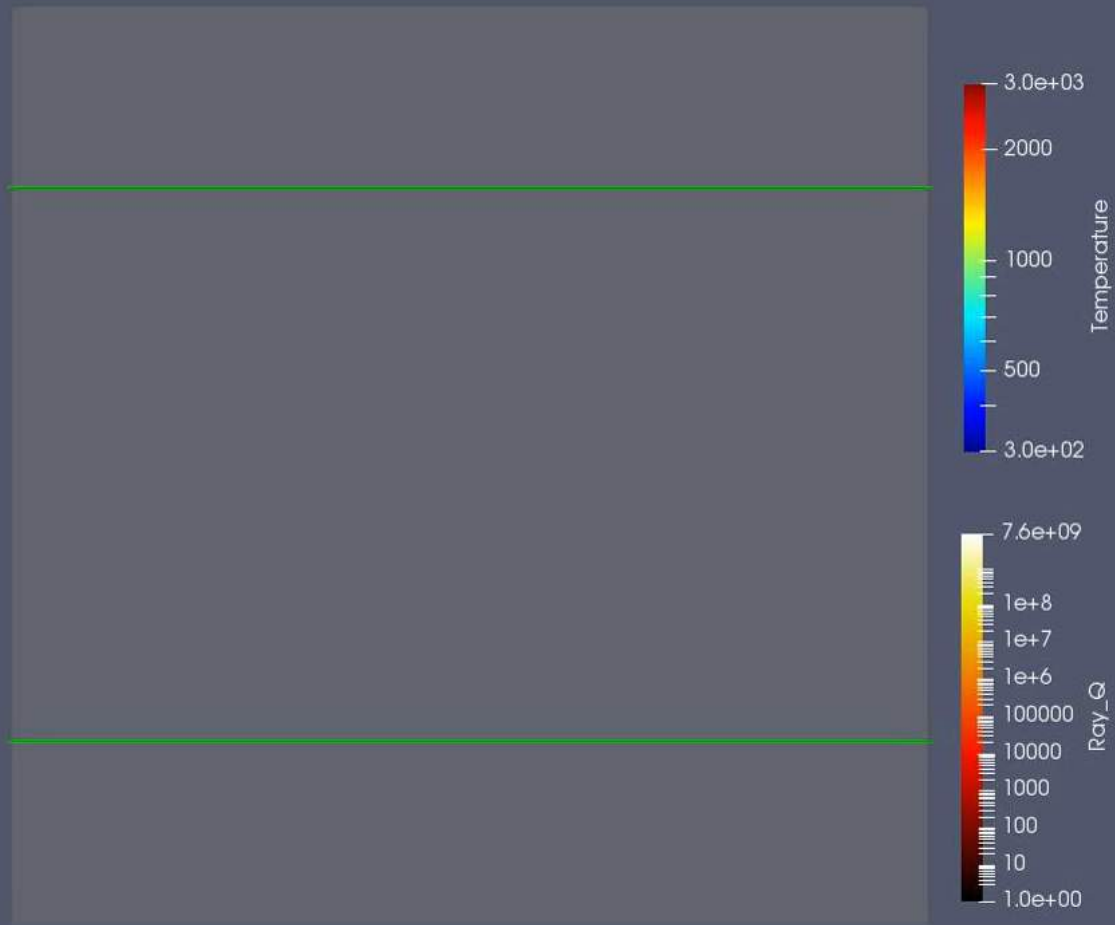


(g) Experimentally observed thermocapillary morphology, re-printed with permission from the work of Cunningham et. al. [20]



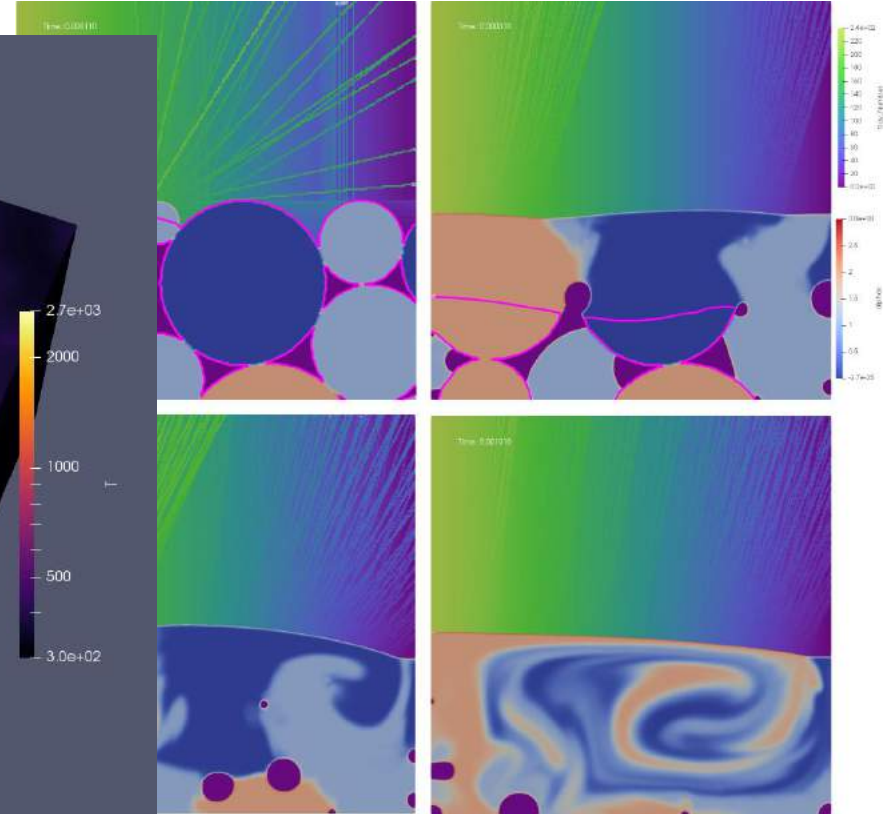
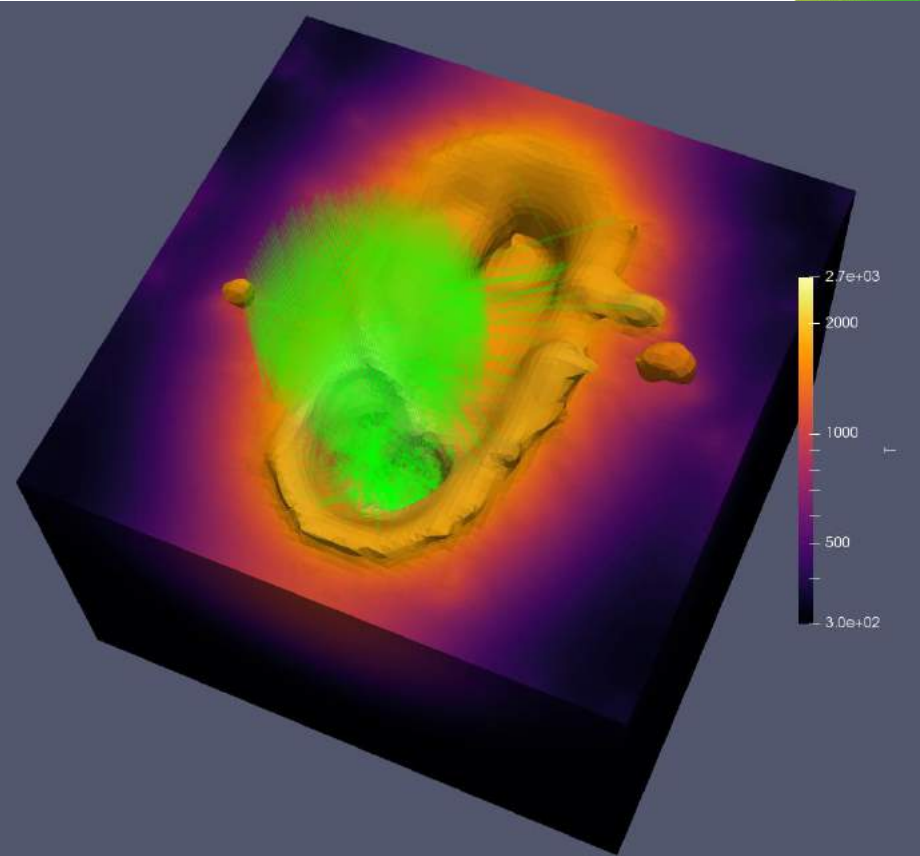
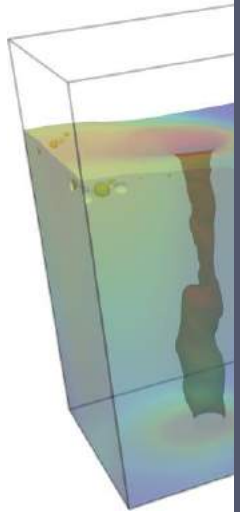
Flint, T. F., Robson, J. D., Parivendhan, G., & Cardiff, P. (2023). laserbeamFoam: Laser ray-tracing and thermally induced state transition simulation toolkit. *SoftwareX*, 21, 101299.





<https://github.com/micmog/LaserbeamFoam>

- Version 2 sources



Flint, T. F., Robson, J. M., and M. J. Heule. 2019. laserbeamFoam: a ray-tracing simulation toolkit.

Magneto-Thermal-Hydrodynamics

Highlights

- Derived a magnetic induction equation describing systems with **gradients in electromagnetic properties**
 - captures internally generated fields due to flow
 - Other formulations are simplified special cases of our formulation – others generally assume **constant properties**
- Our approach also allows numerically stiff terms in the induction equation to be **treated implicitly**
 - Permitting larger time-steps and the simulation of representative systems
- A complete description of flow in advanced manufacturing processes driven by electromagnetic fields** – e.g. arc welding, WAAM etc.

$$\frac{\partial(\rho\mathbf{U})}{\partial t} + \nabla \cdot (\rho\mathbf{U} \otimes \mathbf{U}) = -\nabla P + \nabla \cdot \boldsymbol{\tau} + (\mathbf{J} \times \mathbf{B}) + \Phi.$$

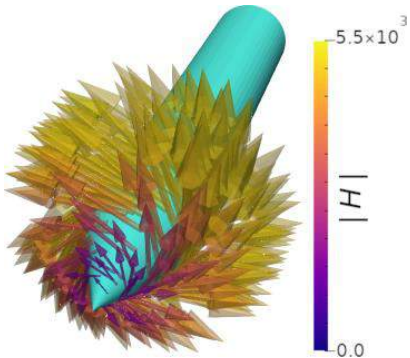
$$\frac{\partial \rho c_p T}{\partial t} + \nabla \cdot (\mathbf{U} c_p \rho T) - \nabla \cdot (k \nabla T) = \frac{\mathbf{J} \cdot \mathbf{J}}{\sigma_E} + S_h$$

$$\frac{\partial(\rho_k \alpha_k)}{\partial t} + \nabla \cdot (\rho_k \alpha_k \mathbf{U}) + \nabla \cdot (\mathbf{U} c \alpha_k (1 - \alpha_k)) = \nabla \cdot \left(\rho D_k \nabla \left(\frac{\rho_k \alpha_k}{\rho} \right) \right)$$

$$\frac{\partial \mu_M \mathbf{H}}{\partial t} - \nabla \cdot [\mu_M (\mathbf{H} \otimes \mathbf{U} - \mathbf{U} \otimes \mathbf{H})] + \nabla \cdot \left[\frac{1}{\sigma_E} (\nabla \mathbf{H}^T - \nabla \mathbf{H}) \right] = 0.$$

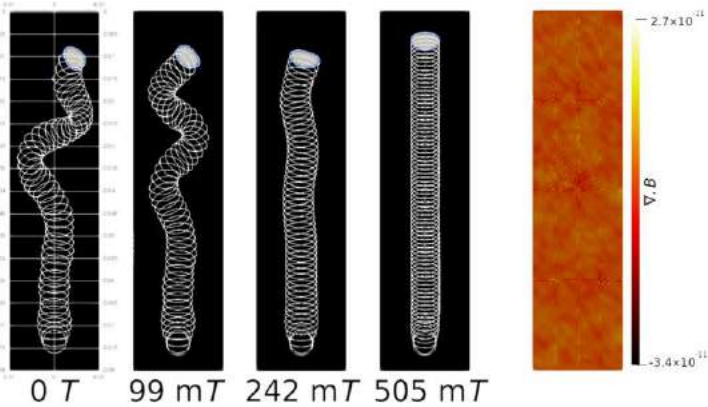
$$\mathbf{B} = \mu_M \mathbf{H}$$

$$\nabla \times \mathbf{H} = \mathbf{J}$$



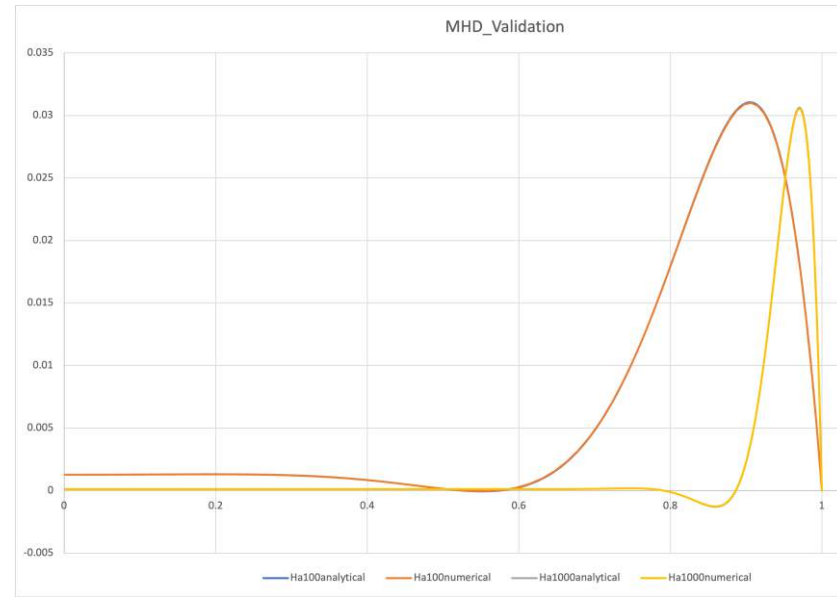
Flint, T.F., Smith, M.C. & Shanthraj, P. Magneto-hydrodynamics of multi-phase flows in heterogeneous systems with large property gradients. *Sci Rep* 11, 18998 (2021).

Magneto- Hydrodynamics

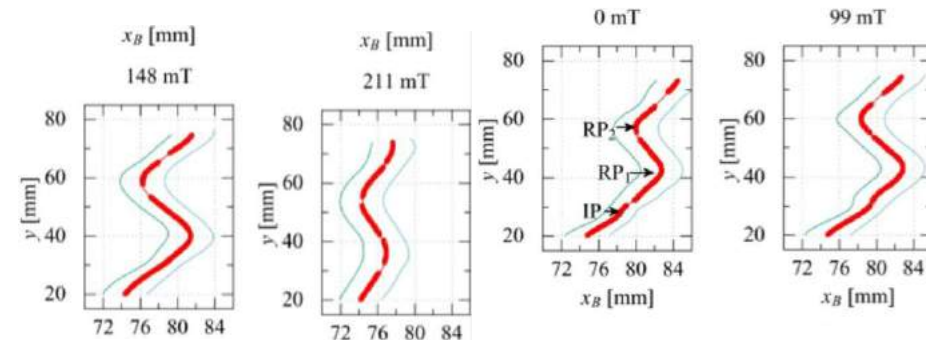


- Validated up to Hartmann numbers of 10000 for single phase problems
- Validated against experimental data with extremely good agreement for multiphase problems

(a) Numerically computed Ar bubble trajectories for the 0 T , 99 mT , 242 mT and 505 mT applied magnetic field cases. Iso-surfaces plotted every $1 \times 10^{-2}\text{ s}$. The divergence of the computed \mathbf{B} field at $t = 0.4\text{ s}$ in the 505 mT case is also shown.



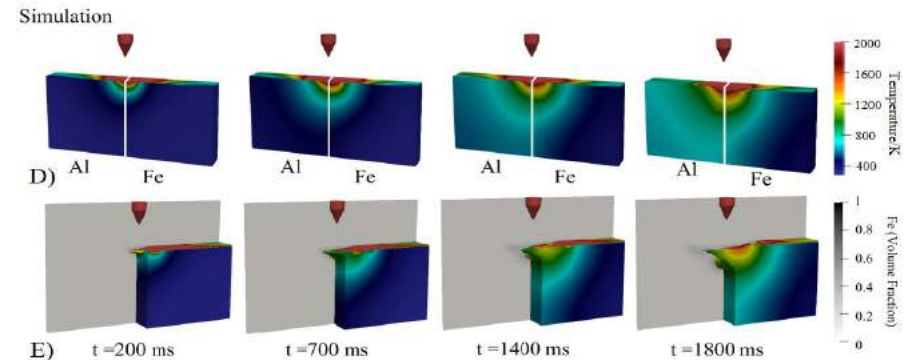
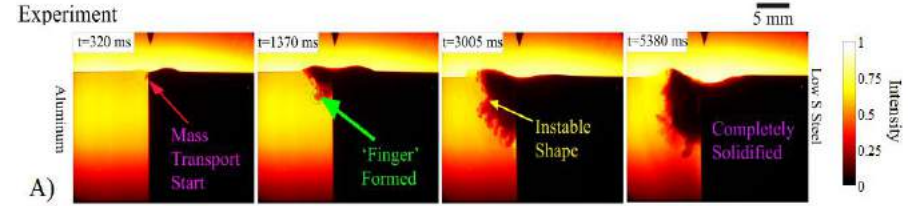
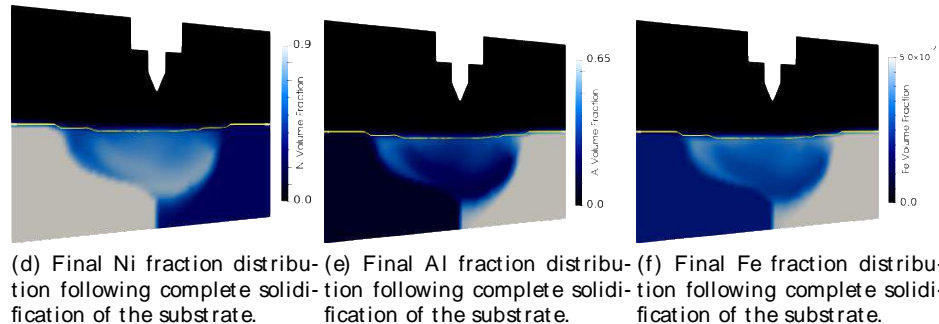
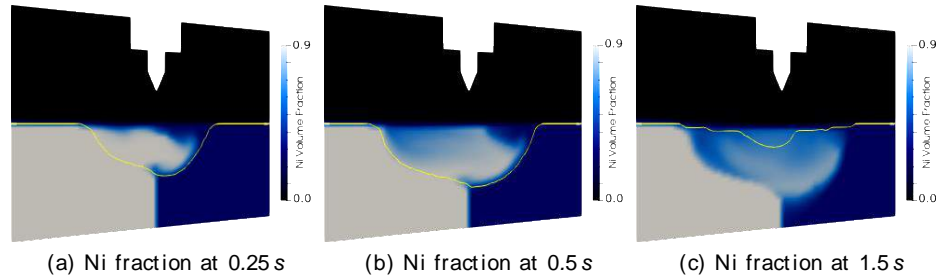
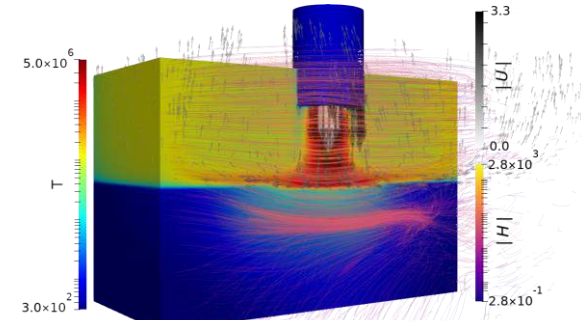
Flint, T.F., Smith, M.C. & Shanthraj, P. Magneto-hydrodynamics of multi-phase flows in heterogeneous systems with large property gradients. *Sci Rep* 11, 18998 (2021).



Magneto-Thermal-Hydrodynamics

Applications: Multi-Component Arc Joining Processes

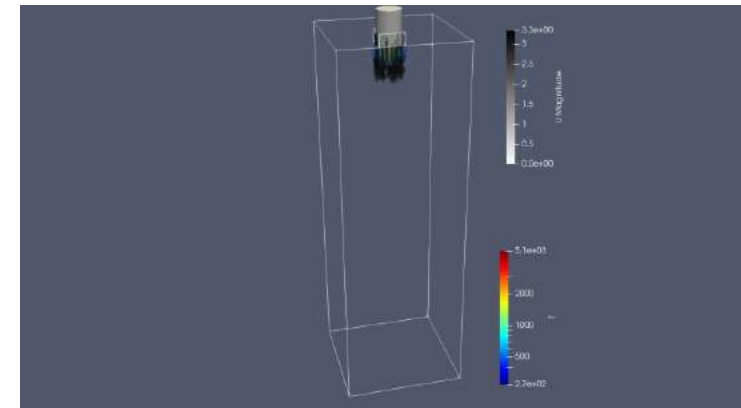
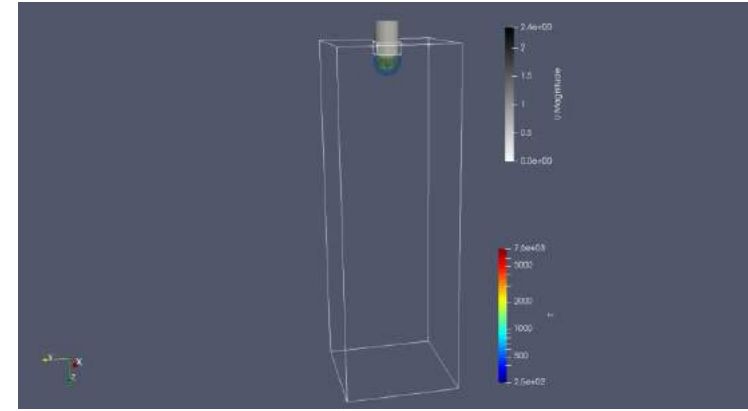
- First complete physics description of arc based joining processes
 - Captures all of the hydrodynamic and electromagnetic physics for a complete predictive capability



Magneto-Thermal-Hydrodynamics

Applications: Tetratics and Plasma Torch Modelling for Glass Sector

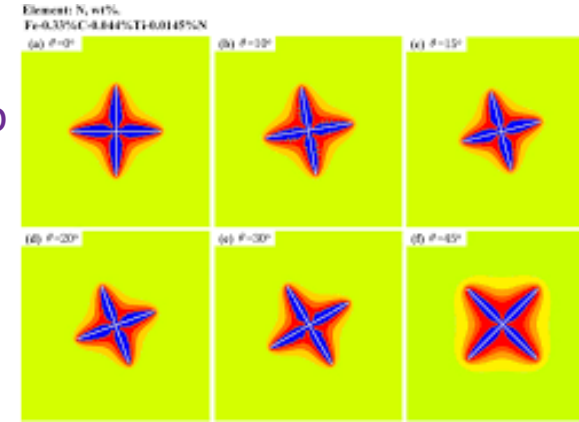
- It turns out that once you capture all the physics – you can apply the same frameworks to different sectors
- Sprint project with Tetratics to demonstrate the power of advanced modelling techniques in plasma torch design for decarbonisation of the glass sector
- Trained a **Royce** application scientist on how to use the numerical implementation
- Investigated fundamental behaviours of plasma in plasma-heating scenarios for the glass sector, specifically Tetratics



Microstructure Modelling

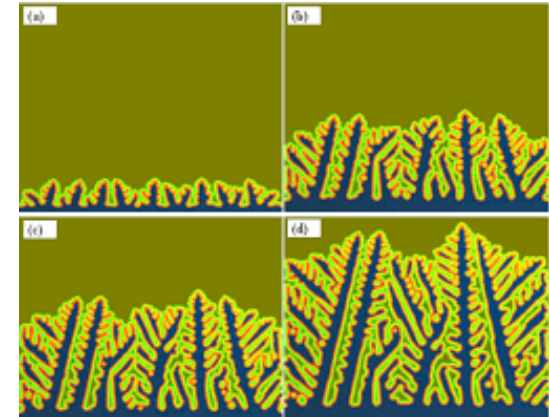
- **Cellular Automata Methods**

- Use simple rules to describe the growth of solid nuclei into liquid melt
- Based on Conways “Game of Life”
- Can re-produce some features of the complex solidification microstructure at the component scale
- Do not contain the driving physics of other higher fidelity approaches



- **Phase-Field Methods**

- The fundamental Physics of phase transformation can more readily be included
- High fidelity approach to understand microstructure evolution



Dynamics

$$\sum_{\alpha} \varphi^{\alpha} = 1, \quad \text{and} \quad \sum_{\alpha} \varphi^{\alpha} x_i^{\alpha} = x_i$$

$$\dot{\varphi}^{\alpha} = - \sum_{\beta=1}^{\tilde{N}} \frac{M^{\alpha\beta}}{\tilde{N}} \left[\frac{\delta \mathcal{F}}{\delta \varphi^{\alpha}} - \frac{\delta \mathcal{F}}{\delta \varphi^{\beta}} \right]$$

$$\dot{x}_i(\tilde{\mu}) + \nabla \cdot (\mathbf{U} x_i) = \nabla \cdot \sum_{j=1}^{K-1} L_{ij}^K \nabla \tilde{\mu}_j$$

$$\frac{\partial(\rho \mathbf{U})}{\partial t} + \nabla \cdot (\rho \mathbf{U} \otimes \mathbf{U}) = -\nabla P + \nabla \cdot \boldsymbol{\tau} + \mathbf{F}_s + \mathbf{F}_g + \mathbf{S}_m$$

$$\frac{\partial \rho c_p T}{\partial t} + \nabla \cdot (\mathbf{U} \rho c_p T) - \nabla \cdot (k \nabla T) = q + S_h$$

True Anisotropic Energy

$$\frac{\delta F}{\delta \phi} = -\nabla \cdot \frac{\partial f}{\partial \nabla \phi} + \frac{\partial f}{\partial \phi}$$

$$\vec{n}_{\alpha\beta} = \frac{\nabla \phi_{\alpha}}{|\nabla \phi_{\alpha}|},$$

$$a = 1 + \epsilon_1 (4(n_x^4 + n_y^4 + n_z^4) - 3)$$

Free Energy

$$\mathcal{F}(\varphi, \nabla \varphi, \mathbf{x}^{\alpha}, T) = \int_V \left(f_{\text{intf}}(\varphi, \nabla \varphi) + f_{\text{bulk}}(\varphi, \mathbf{x}^{\alpha}, T) \right) dV,$$

$$f_{\text{intf}}(\varphi, \nabla \varphi) = \sum_{\alpha \neq \beta}^N \frac{4\sigma^{\alpha\beta}}{\eta^{\alpha\beta}} \left[-\frac{\eta^{\alpha\beta^2}}{\pi^2} \nabla \varphi^{\alpha} \cdot \nabla \varphi^{\beta} + \varphi^{\alpha} \varphi^{\beta} \right]$$

$$\Omega f_{\text{chem}}^{\alpha} = A^{\alpha} + \sum_{i=1}^{K-1} B_i^{\alpha} x_i + \frac{1}{2} \sum_{i=1}^{K-1} \sum_{j=1}^{K-1} C_{ij}^{\alpha} x_i x_j + RT \sum_{i=1}^K x_i \ln(x_i)$$

$$f_{\text{chem}}(\varphi, \mathbf{x}^{\alpha}, T) = \sum_{\alpha} \varphi^{\alpha} f_{\text{chem}}(\mathbf{x}^{\alpha}, T)$$

$$\Delta G^{\alpha\beta} = - \left[\frac{\partial f_{\text{chem}}}{\partial \varphi^{\alpha}} - \frac{\partial f_{\text{chem}}}{\partial \varphi^{\beta}} \right]$$

$$= f_{\text{chem}}^{\beta}(\mathbf{x}^{\beta}) - f_{\text{chem}}^{\alpha}(\mathbf{x}^{\alpha}) - \sum_{i=1}^{K-1} \left[\tilde{\mu}_i \left(x_i^{\beta}(\tilde{\mu}^{\beta}, T) - x_i^{\alpha}(\tilde{\mu}^{\alpha}, T) \right) \right]$$

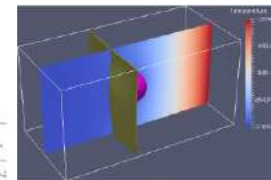
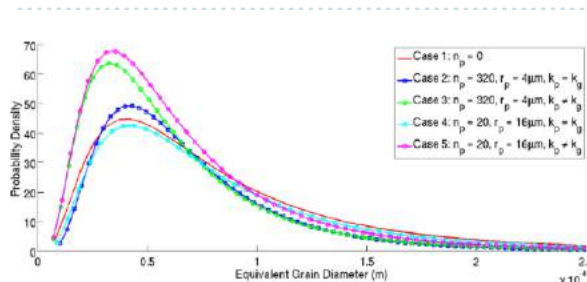
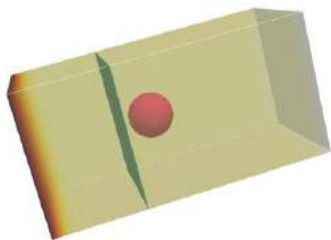
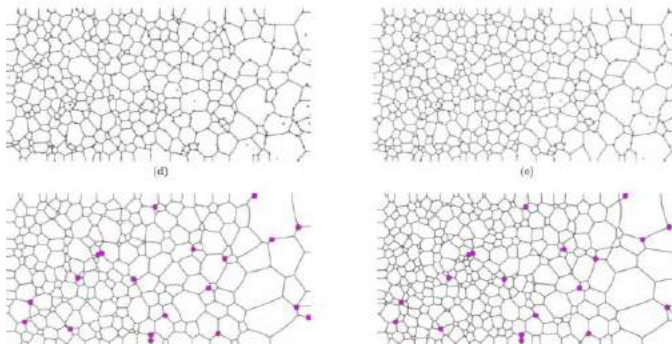
Kinetics

$$L_{ij}^K = \sum_{\alpha=1}^N \varphi^{\alpha} {}^{\alpha} L_{ij}^K$$

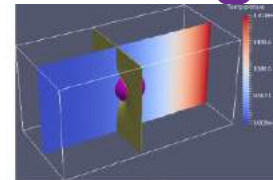
$${}^{\alpha} L_{ij}^K = \sum_{l=1}^K (\delta_{jl} - x_j^{\alpha}) (\delta_{li} - x_i^{\alpha}) x_i^{\alpha} M_l^{\alpha}$$

Applications: HAZ microstructure evolution effect of conductivity

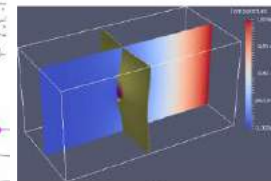
- Modelling permits meaningful investigations into the evolution of microstructure in HAZ: Heterogeneous thermal properties of second phase particles



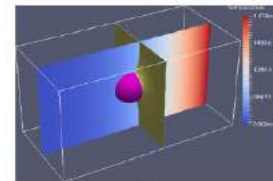
(a)



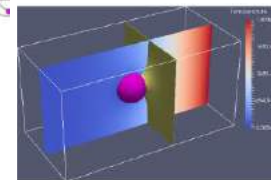
(b)



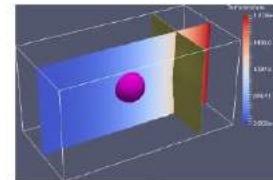
(c)



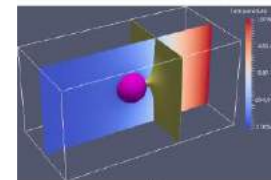
(d)



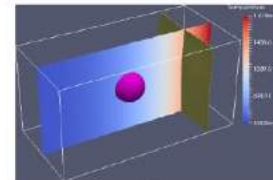
(e)



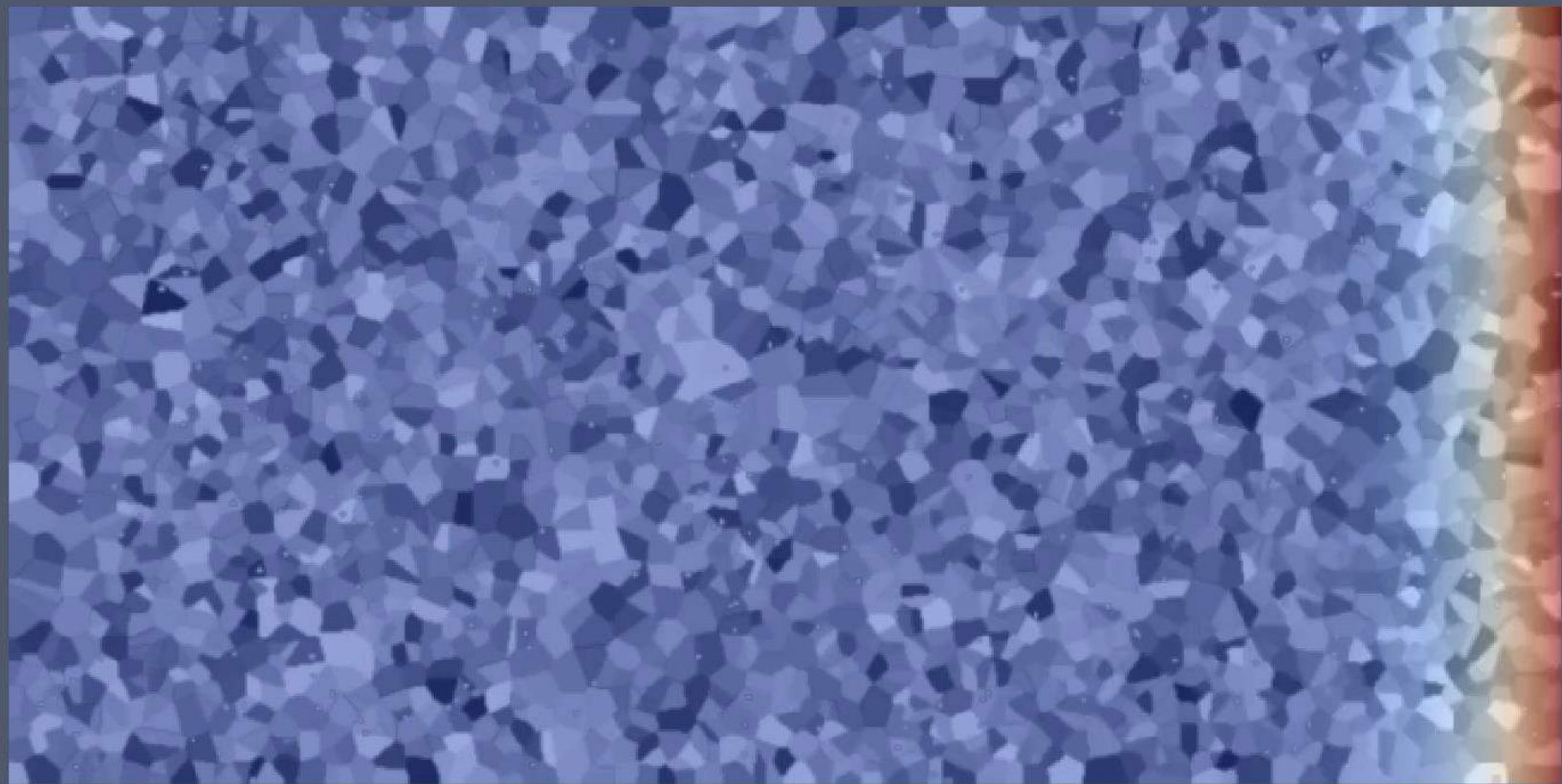
(f)



(g)



(h)

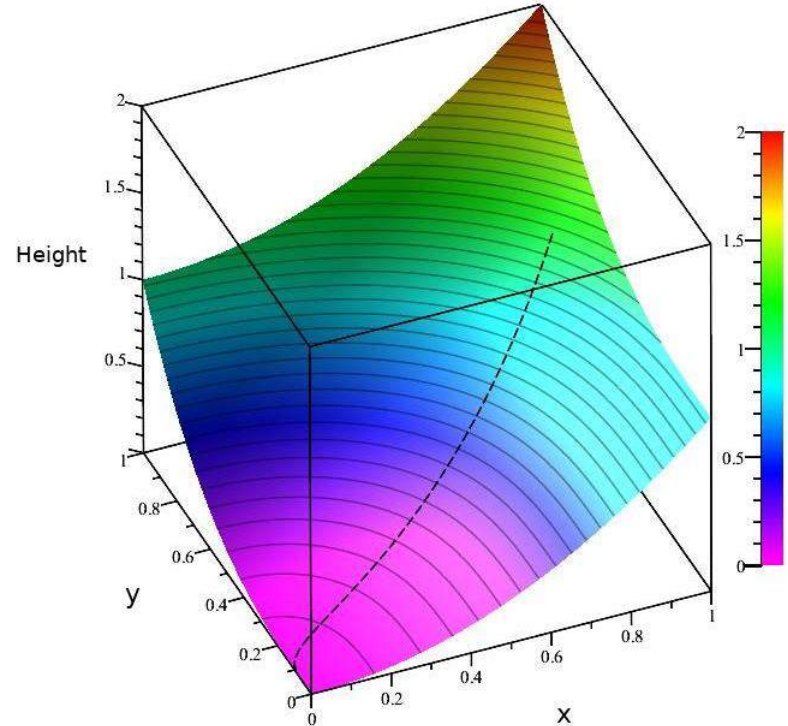


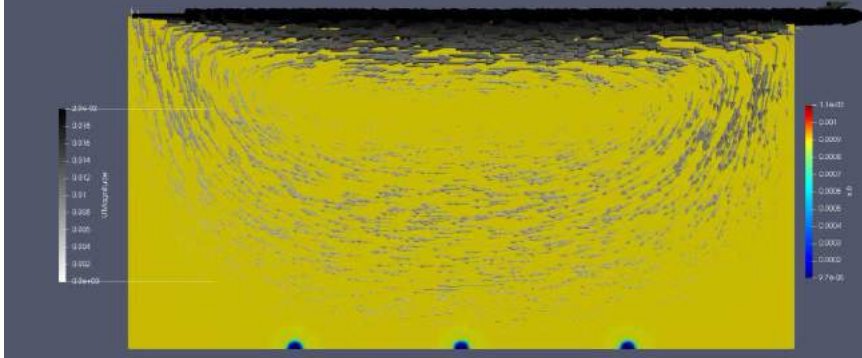
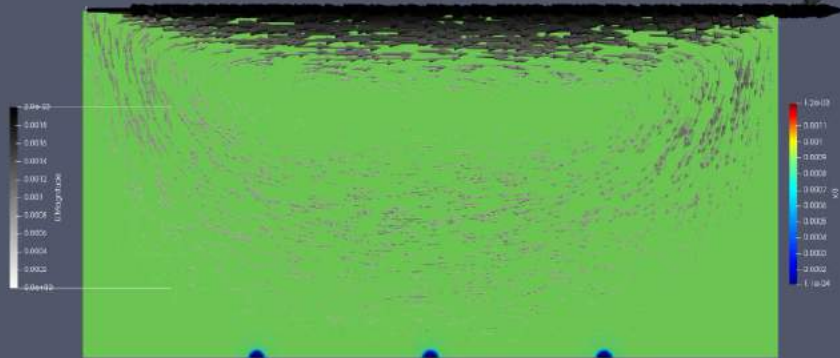
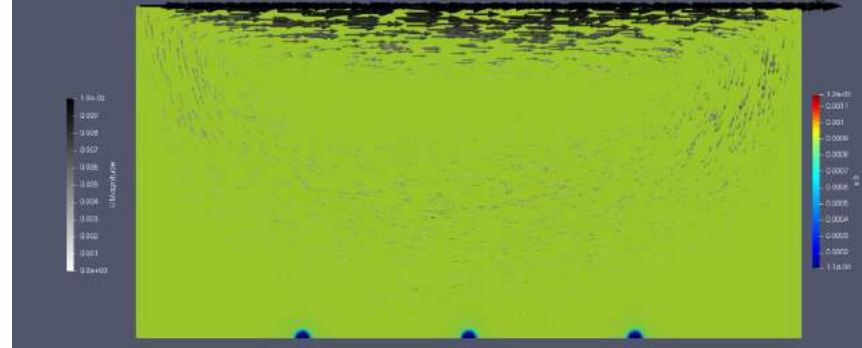
Phase-Field Treatment of Interface Anisotropy

- Phase-Field Modelling is all about finding the most efficient path down a hill – or Free-Energy Landscape – to minimise the global free energy
- Mathematically this means $\frac{\delta F}{\delta \phi} = -\nabla \cdot \frac{\partial f}{\partial \nabla \phi} + \frac{\partial f}{\partial \phi}$.
- With Alloy Solidification the energy term now strongly depends on the gradient in the phase field variable – i.e. the normal vector at the liquid/solid interface
 - For Cubic materials this is to the power 4
 - Makes the free energy minimisation “non-trivial”
 - Others neglect this.....I wonder why....

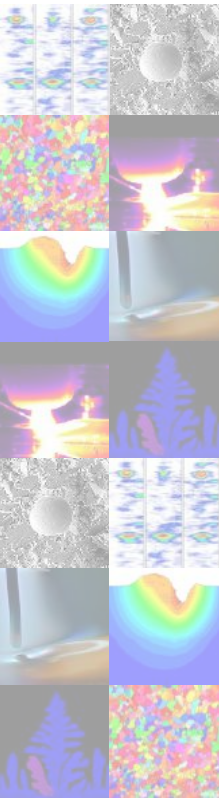
$$\vec{n}_{\alpha\beta} = \frac{\nabla \phi_\alpha}{|\nabla \phi_\alpha|}$$

$$a = 1 + \epsilon_1 (4(n_x^4 + n_y^4 + n_z^4) - 3)$$





Continuum Field Phase Field Modeling



CFD: $\frac{\partial(\rho U)}{\partial t} + \nabla \cdot (\rho U \otimes U) = -\nabla P + \nabla \cdot \tau + F_s + F_g + S_m$

$$\nabla \cdot U = 0$$

Surface Tension $F_s = \left[(\sigma \kappa + P_v) \hat{n} + \frac{d\sigma}{dT} (\nabla T - (\hat{n} \cdot \nabla T) \hat{n}) \right] |\nabla \alpha|$

Volume of Fluid $\frac{\partial \alpha}{\partial t} + \nabla \cdot (\alpha U) = 0$

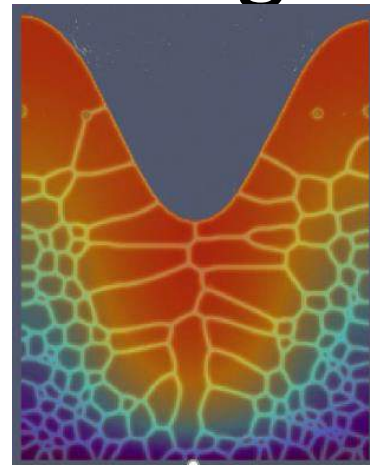
Conservation of Energy $\frac{\partial \rho c_p T}{\partial t} + \nabla \cdot (U \rho c_p T) - \nabla \cdot (k \nabla T) = q + S_h$

Phase Field $\frac{\partial \xi}{\partial t} = -L_P \frac{\delta F}{\delta \xi} \quad \frac{\partial \eta_i}{\partial t} = -L_G \frac{\delta F}{\delta \eta_i}$

$$f_{phase} = m_p \left\{ (1 - \xi)^2 \phi + \xi^2 (1 - \phi) \right\} \quad f_{gradient} = \frac{\kappa_p}{2} (\nabla \xi)^2 + \frac{\kappa_g}{2} (\nabla \eta_i)^2$$

$$f_{grain} = m_g \left\{ \sum_{i=1}^n \left(\frac{\eta_i^4}{4} - \frac{\eta_i^2}{2} \right) + \gamma \sum_{i=1}^n \sum_{j \neq i} \eta_i^2 \eta_j^2 + \frac{1}{4} (1 - \xi)^2 \sum_{i=1}^n \eta_i^2 \right\} \quad F = \int_V (f_{phase} + f_{grain} + f_{gradient}) dV$$

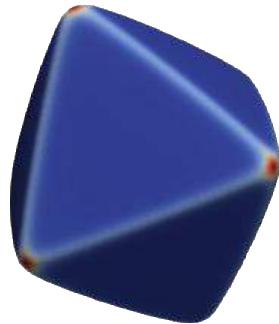
Nuc $\Delta T_{nuc} \sim \mathcal{N}(\Delta T_{nuc\mu}, \Delta T_{nuc\sigma}^2)$



- Code is ready for release
- Paper is mostly written
- Just need to run high mesh resolution test cases, include the results in the paper and discuss.

Capabilities:

- **Preferred crystallographic growth directions**
 - Cheap but effective method to include crystallographic orientation
 - Anisotropy introduced in grain boundary mobility, but not surface energy (v. expensive)
- **Grain Coarsening**
- **Heterogenous nucleation**
- **Laser ray-tracing heat source: L-PBF**
- **Powder substrate included.**
- **Latent Heat Conservation**



software



Demonstration Cases:

1. Aniso_Solidification

- Orientation dependant competitive growth of columnar grains in a thermal gradient

2. NucTestCase

- Heterogenous nucleation and grain coarsening

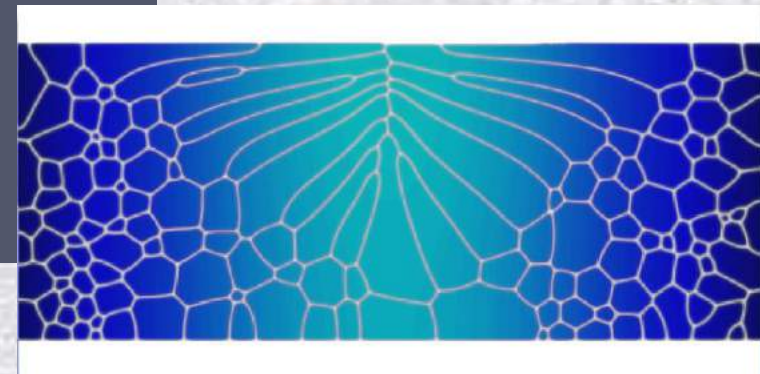
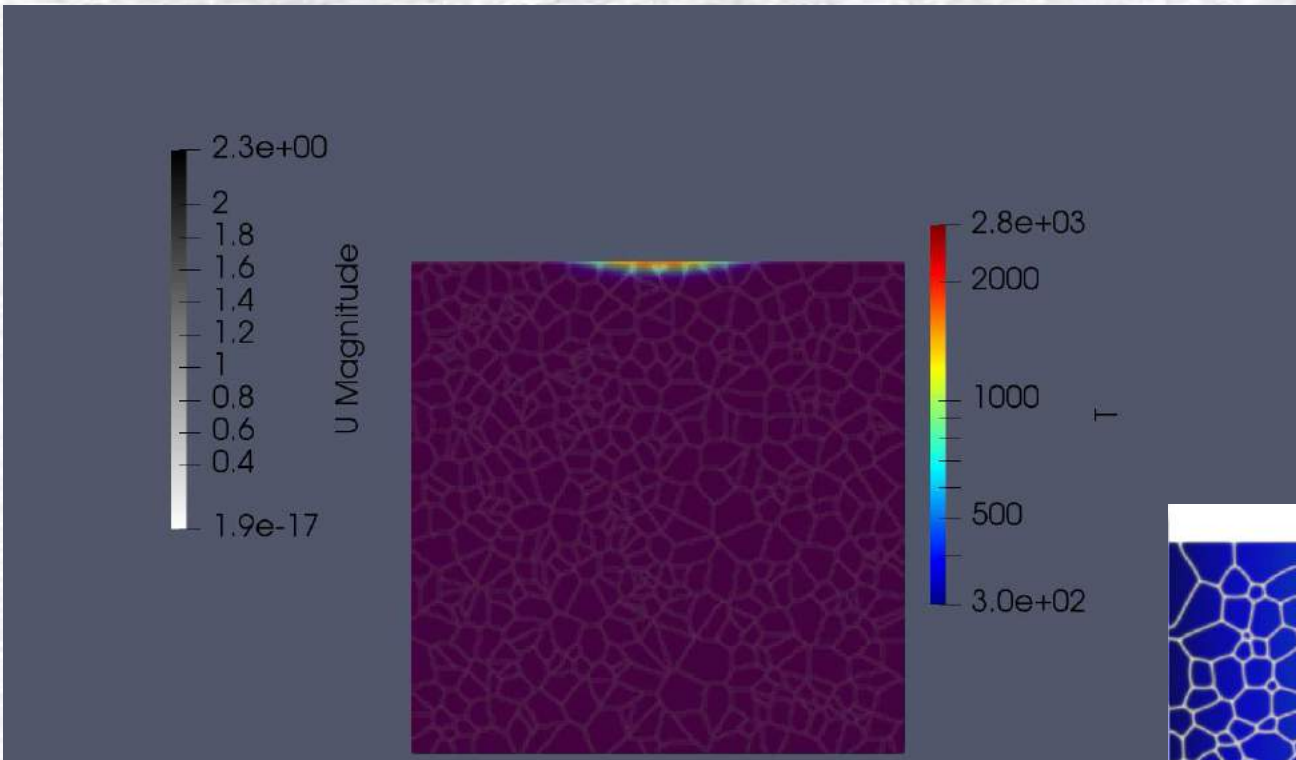
3. PowderBed

- L-PBF single track melting and solidification
- Powder substrate
- Ray tracing heat source

4. KeyholeWeld

- Deep keyhole formation and solidification

Single Component Multi-Phase Field Approach (microstructureFoam)



Core principle in continuum mechanics is the conservation of various quantities

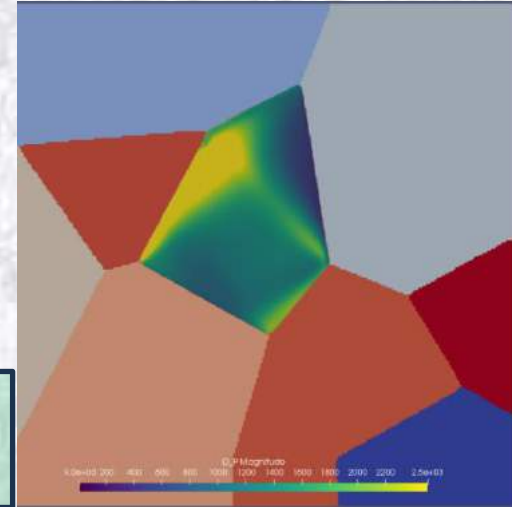
$$\frac{\partial \rho}{\partial t} + \nabla \cdot (\rho \mathbf{U}) = 0 \quad \text{Conservation of Mass}$$

$$\frac{\partial (\rho \mathbf{U})}{\partial t} + \nabla \cdot (\rho \mathbf{U} \otimes \mathbf{U}) - \nabla \cdot \boldsymbol{\sigma} = 0 \quad \text{Conservation of Momentum}$$

$$\frac{\partial (\rho E)}{\partial t} + \nabla \cdot (\rho \mathbf{U} E) - \nabla \cdot (\boldsymbol{\sigma} \cdot \mathbf{U}) - \nabla \cdot (\kappa \nabla T) = 0 \quad \text{Conservation of Energy}$$

$$E = e(T) + \frac{\mathbf{U}^2}{2} \quad \text{with } e(T) = C_v T$$

We consider a material with Eulerian velocity $\mathbf{U}(x, t)$ and Cauchy stress tensor $\boldsymbol{\sigma}(x, t)$. The total velocity gradient tensor, $\mathbf{L} = \nabla \mathbf{U}$ is additively decomposed into elastic and plastic parts: $\mathbf{L} = \mathbf{L}^e + \mathbf{L}^p$, as well as into rate of deformation, $\mathbf{D} = \nabla \mathbf{U}^{symm}$, and rate of rotation (spin), $\boldsymbol{\Omega} = \nabla \mathbf{U}^{skew}$, respectively.



$$\mathbf{D} = \mathbf{D}^e + \mathbf{D}^p, \quad \boldsymbol{\Omega} = \boldsymbol{\Omega}^e + \boldsymbol{\Omega}^p$$

The rate of deformation, and rate of rotation are decomposed additively into elastic (reversible) and plastic (irreversible) contributions

The macroscopic plastic velocity gradient links different scales of the problem, and considers activation of crystal slip-systems. The plastic velocity gradient is expressed as the superposition of shear deformation caused by crystallographic slip, per order-parameter.

$$\mathbf{L}_i^p = \sum_{\alpha} \dot{\gamma}_i^{\alpha} \mathbf{S}_i^{\alpha} \quad \mathbf{S}_i^{\alpha} = m_i^{\alpha} \otimes n_i^{\alpha} \quad \tau_i^{\alpha} = \boldsymbol{\sigma} : \mathbf{S}_i^{\alpha}$$

Resolved shear stress: stress in each slip-system

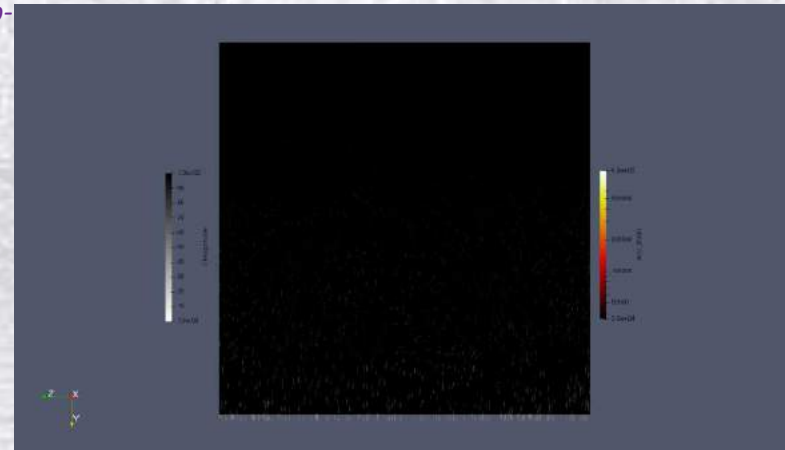
$$\dot{\gamma}_i^{\alpha} = \dot{\gamma}_0 \left(\frac{|\tau_i^{\alpha}|}{g_i^{\alpha}} \right)^k \text{sgn}(\tau_i^{\alpha})$$

$$\mathbf{D}_i^p = \frac{1}{2} \left(\mathbf{L}_i^p + \mathbf{L}_i^{pT} \right) = \sum_{\alpha} \dot{\gamma}_i^{\alpha} \mathbf{p}_i^{\alpha}$$

$$\boldsymbol{\Omega}_i^p = \frac{1}{2} \left(\mathbf{L}_i^p - \mathbf{L}_i^{pT} \right) = \sum_{\alpha} \dot{\gamma}_i^{\alpha} \boldsymbol{\omega}_i^{\alpha}$$

$$\mathbf{p}_i^{\alpha} = \frac{1}{2} \left(m_i^{\alpha} \otimes n_i^{\alpha} + n_i^{\alpha} \otimes m_i^{\alpha} \right)$$

$$\boldsymbol{\omega}_i^{\alpha} = \frac{1}{2} \left(m_i^{\alpha} \otimes n_i^{\alpha} - n_i^{\alpha} \otimes m_i^{\alpha} \right)$$



- We then consider an ensemble of N grains in a poly-crystal aggregate
- Each grain/phase may plastically deform on its unique slip systems in its local reference frame
- Convert from local to global reference frame through a rotation matrix, R

$$\mathbf{R}_i = \begin{pmatrix} \cos \chi_i \cos \psi_i & \sin \theta_i \sin \chi_i \cos \psi_i - \cos \theta_i \sin \psi_i & \cos \theta_i \sin \chi_i \cos \psi_i + \sin \theta_i \sin \psi_i \\ \cos \chi_i \sin \psi_i & \sin \theta_i \sin \chi_i \sin \psi_i + \cos \theta_i \cos \psi_i & \cos \theta_i \sin \chi_i \sin \psi_i - \sin \theta_i \cos \psi_i \\ -\sin \chi_i & \sin \theta_i \cos \chi_i & \cos \theta_i \cos \chi_i \end{pmatrix}$$

$$\mathbb{C}_i = \mathbf{R}_i \cdot \mathbf{R}_i \cdot \mathbb{C}'_{i_mnpq} \cdot \mathbf{R}_i \cdot \mathbf{R}_i$$

$$m_i^\alpha = \mathbf{R}_i \cdot m_i^{\alpha'}$$

$$n_i^\alpha = \mathbf{R}_i \cdot n_i^{\alpha'}$$

- We have relationships that relate the slip rates on all slip systems to the hardening between slip-systems

$$h_i^\beta = h_{0_i} \operatorname{sech}^2 \left(\frac{h_{0_i} \gamma_i^\alpha}{\tau_{s_i} - \tau_{0_i}} \right) \qquad \dot{g}_i^\alpha = \sum_{\beta} h_i^{\alpha\beta} |\dot{\gamma}_i^\beta|$$

- Finally, we can relate the rate of deformation to the stress rate through the 4th order stiffness tensor of each grain/phase in its local reference frame
- It is essential for the rate dependent elastic–plastic constitutive equation to be frame invariant (or objective); however, frame invariance of the stress rate is not guaranteed even if the strain rate is frame invariant
- The stress rate in all phases is computed using the Jaumann rate, given by:

$$\check{\sigma}_i = \mathbb{C}_i : (D - D_i^p) - \sigma \operatorname{tr}(D - D_i^p) = \dot{\sigma}_i + (\sigma \cdot (\Omega - \Omega_i^p) - (\Omega - \Omega_i^p) \cdot \sigma)$$

$$\dot{\sigma} = \sum_i^M \varphi_i \dot{\sigma}_i$$

$$\check{\sigma}_i = \mathbb{C}_i : (D - D_i^p) - \sigma \text{tr} (D - D_i^p) = \dot{\sigma}_i + (\sigma \cdot (\Omega - \Omega_i^p) - (\Omega - \Omega_i^p) \cdot \sigma)$$

- Use a diffuse interface description: need to average the stress rates by the volume fraction of each phase present at a given location

$$\dot{\sigma} = \sum_i^M \varphi_i \dot{\sigma}_i$$

As we are concerned with the Eulerian frame of reference these orientation fields, θ_i , χ_i and ψ_i must be advected through the domain, and updated by the appropriate components of the corresponding elastic spin tensor, $\Omega_i^e = \Omega - \Omega_i^p$, that describe rotation around each axis:

- The local orthonormal basis of each material point is then updated by the elastic part of the spin tensor
- It can be shown that the expansion of the matrix exponential used to solve these rate equations can be analytically found with a 3rd order series expansion
- For computational tractability, we then find the euler angles corresponding to the elastic rotation matrix and advect these three fields (per phase)

- Other fields that describe material point information must also be advected, including the order parameter fields, and slip-system fields:

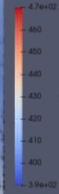
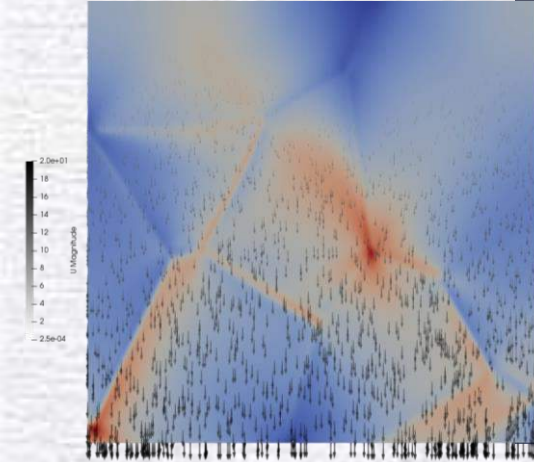
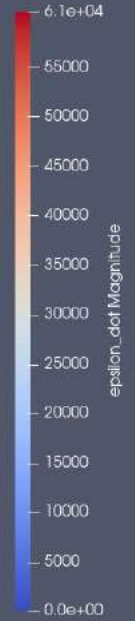
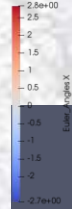
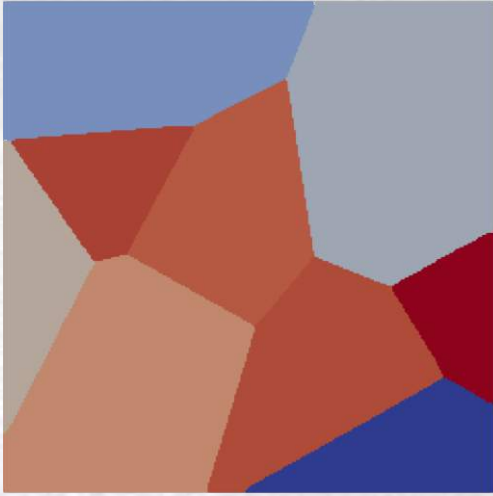
$$\frac{\partial \rho \varphi_i}{\partial t} + \nabla \cdot (\rho \mathbf{U} \varphi_i) = 0$$

$$\frac{\partial \rho g_i^\alpha}{\partial t} + \nabla \cdot (\rho \mathbf{U} g_i^\alpha) = (\rho \dot{g}_i^\alpha)$$

$$\frac{\partial \rho \gamma_i^\alpha}{\partial t} + \nabla \cdot (\rho \mathbf{U} \gamma_i^\alpha) = (\rho \dot{\gamma}_i^\alpha)$$

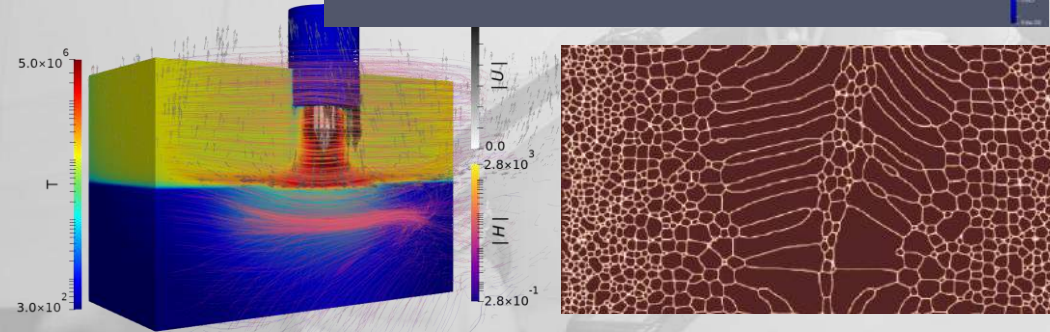
- This completes our system of equations that fully describes high strain rate deformation in a Eulerian frame of reference, for poly-crystalline and multi-component multi-phase materials
- The substrate can be any number of phases, with any number of slip systems (e.g. alpha – beta microstructure, mixture of HCP and BCC phases etc)

Solid Mechanics and Solid Dynamics Work: Eulerian Crystal Plasticity



- If we want a truly predictive mathematical framework – we have to include all of the physics, at least in the first instance
- At Manchester we have developed the most mathematically rigorous, and physically robust descriptions of:
 - **Multi-Component fusion and vapourisation:** preferential element loss, true keyhole stability analysis
 - **Multi-Component MHD with property gradients:** Full physics simulation of arc based processes (e.g. Alternating Current, not possible previously), Fusion plasma collapse
 - **Multi-Component laser-substrate interaction:** multiple reflections of laser source within keyhole
 - **Multi-Phase, Multi-Component, Phase Field Frameworks:** prediction of solidification and HAZ microstructure formation, phase transformations
 - Developing Eulerian **high strain-rate Poly-Crystal-Plasticity** frameworks
- Strong advocates for **open-science** and **open-source** modelling software
 - MatFlow, laserbeamFoam, HEDSATS, PRISMS-PF,.....

Thankyou for the opportunity
I'd love to answer any questions



Dr Tom Flint (Left)
Tom.Flint@Manchester.ac.uk